LAWRENCE
LIVERMORE
NATIONAL
LABORATORY

UCRL-PROC-236247

Effect of Random Clustering on Surface Damage Density Estimates

M. J. Matthews, M. D. Feit

November 6, 2007

SPIE - Boulder Damage Symposium
Boulder, CO, United States
September 24, 2007 through September 26, 2007

Disclaimer

Effect of Random Clustering on Surface Damage Density Estimates

Manyalibo J. Matthews and Michael D. Feit
Lawrence Livermore National Laboratory, 7000 East Avenue, Livermore, CA 94550

ABSTRACT

Identification and spatial registration of laser-induced damage relative to incident fluence profiles is often required to characterize the damage properties of laser optics near damage threshold. Of particular interest in inertial confinement laser systems are large aperture beam damage tests (>1cm^2) where the number of initiated damage sites for ϕ>14J/cm^2 can approach 10^5-10^6, requiring automatic microscopy counting to locate and register individual damage sites. However, as was shown for the case of bacteria counting in biology decades ago, random overlapping or 'clumping' prevents accurate counting of Poisson-distributed objects at high densities, and must be accounted for if the underlying statistics are to be understood. In this work we analyze the effect of random clumping on damage initiation density estimates at fluences above damage threshold. The parameter $\psi=a\rho=\rho/\rho_0$, where $a=1/\rho_0$ is the mean damage site area and ρ is the mean number density, is used to characterize the onset of clumping, and approximations based on a simple model are used to derive an expression for clumped damage density vs. fluence and damage site size. The influence of the uncorrected ρ vs. ϕ curve on damage initiation probability predictions is also discussed.

INTRODUCTION

The damage threshold of optics used in inertial confinement fusion (ICF) lasers, where laser fluence can average more than 8 J/cm^2, is a key parameter used to predict the expected lifetime of the ICF optics [1]. By exposing numerous spots on an optic with a range of pulse energies from a focused laser beam, such as in a so-called S/1 or R/1 test, damage thresholds can be ascertained by analyzing the resulting S-curve. In general, the 1/e^2 laser spot size is in the range of microns to ~1mm, which means that a large number of sample areas must be taken to obtain reasonable statistics. Furthermore, some may argue that probing an optic with a small beam is not a realistic test of an optic used in large aperture laser systems. An alternative damage test involves a moderate aperture (~2 cm^2) beam with sufficient contrast to access fluences above and below damage threshold. Spatial registration of the laser beam footprint and the resulting damage allows one to infer a damage density versus fluence, or $\rho(\phi)$ vs. ϕ, curve, where the damage probability of a particular area can be found using Poisson statistics. The '$\rho(\phi)$ vs. ϕ' damage test method has the ability of measuring the mean density of all initiators versus fluence and the probability can be calculated for different test areas, and thus can be, in this regard, considered more advantageous in terms of probability calculations than small area S/1 testing.

Because of the large number of damage sites created by ~cm sized aperture laser pulses (for example, a fused silica surface exposed to a ~20 J/cm^2 mean fluence with 15% contrast may create as many as 100,000 damage initiations), automated microscopy is needed for damage site counting. This entails –raster-imaging areas exposed to the laser pulse with appropriate lighting and resolution (usually backlighting and NA>0.1), setting a threshold whereby the background can be distinguished from the damaged area, and registering the coordinates of each object above an image grey-value threshold. Through the use of beam and sample fiducials, micron-level registration of the fluence to the damage coordinates can (in principle) be achieved, yielding the usual exponential or power-law curves for $\rho(\phi)$ vs. ϕ. However, as the density of damage increases, the number of damage sites that overlap, or 'clump' within the damaged area, prevents accurate counting of individual initiations using automatic scanning techniques. At such high fluences where densities reach this limit, one is no longer measuring the $\rho(\phi)$ vs. ϕ of damage initiations, but rather the $\rho(\phi)$ vs. ϕ of damage initiation clumps.

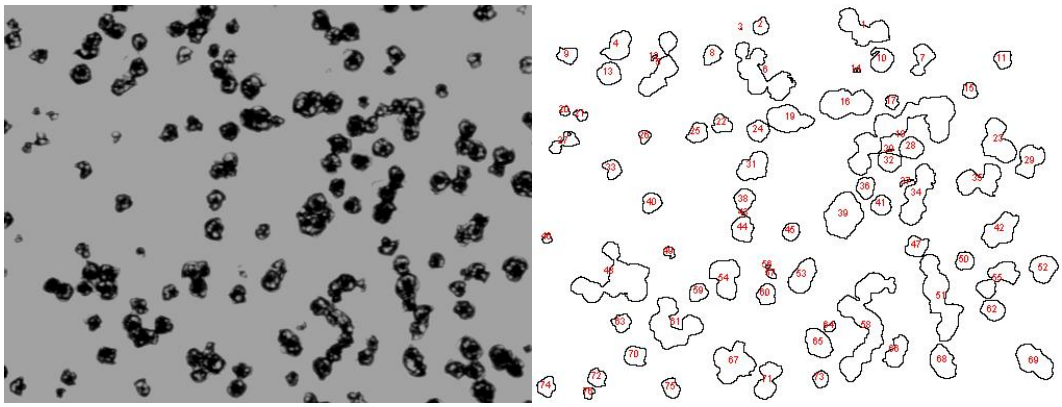

Figure 1: (left) An optical micrograph (5x/0.2NA, back-illuminated) showing the spatial distribution of damage sites produced by a ~18 J/cm^2 portion of a 2-cm diameter, 3ns Gaussian pulse. (right) Outlines showing the result of thresholding the image in (b), which correspond to the individual detections of 'blobs' which in several cases is associated with clusters/clumps of damage sites, and not individual sites.

It is known that objects of finite spatial extent placed at random in space will have a probability of overlap based on their size and the spatial extent over which they are distributed. This is true in all dimensions, and several examples can be found in various fields of science. In one dimension, a segment can be sub-divided into finite length parts or two or more types, and one may ask what the probability is for any type to appear consecutively given the total number of types and sub-divisions. Such a question is important in queuing theory and applicable to computation and networking where 'bits' form the segments in the queue[2]. In two dimensions, lamina may be placed at random in a plane, such as poker chips on a table, and the question of overlap can be similarly investigated. Many practical examples of 2-D clumping, in fact, have been available for decades, ranging from 'strategic' aerial bombing during WW II involving bombs placed at random over a target area[3], to the study of randomly distributed bacteria colonies in a Petri dish[4]. Percolation theory in transport physics can be viewed as an extreme example of clumping in 2- or 3-D when an electronic path is created by the overlap of randomly-connected conducting particles or crystallites[5].

In this paper we review the theory of 'random clumping' and apply a simple model to explain the behavior of the measured $\rho(\phi)$ vs. ϕ at high-ϕ for fused silica surface damage as clumping of damage becomes important. Using a Weibull distribution for damage site initiation at low densities, and a simple Poisson-based model for clumping at high densities, we construct a functional form of $\rho(\phi)$ that can be used to show how clumping affects $\rho(\phi)$ vs. ϕ as a function of both the intrinsic ρ and damage site size. Finally, we show as an example how damage expectation predictions are influenced by changes in $\rho(\phi)$ caused by clumping, and in particular the influence on the study of damage caused by spatial hotspots in a laser beam.

OVERLAP OF RANDOMLY PLACED OBJECTS IN TWO DIMENSIONS

In order to estimate the amount of under-counting involved in automated threshold-imaging microscopy due to clumping of individual damage sites, we start by describing the probability of observing a clump of *n* sites if the total number and areal density of sites is given by N and ρ_N respectively. (A more complete description of this approximation can be found in Roach [6]) For simplicity, we assume each site is circular, and has a diameter δ (which will be argued later as a justifiable assumption). Under Poisson statistics, the probability that a single damage site is not overlapped by any other randomly placed site is just the probability that no other site has its center within a diameter distance:

$$p_0 = \exp(-\pi\delta^2\rho_N)\,. \tag{1}$$

It follows that the probability of any site existing within an area $\pi\delta^2$ and overlapping a given site is $1-p_0$. We then 'build' an *n*-membered clump by requiring that, as we search outward from any site to its nearest neighbor, the inter-site distance be less than 2δ, and similarly the distance between that site and its nearest neighbor be less than 2δ, until we reach the last site which resides at a distance from the next progressive nearest neighbor greater than 2δ. The probability of observing this chain of *n* sites is can be approximated by the probability of *n*-1 overlapped sites followed by 1 isolated site, or

$$p_n = p_0(1 - p_0)^{n-1} \tag{2}$$

such that the mean density of isolated *n*-membered clumps given a mean site density ρ_N is approximately given by

$$\rho_N \frac{p_n}{n} = \rho_N \frac{p_0(1-p_0)^{n-1}}{n}. \tag{3}$$

The mean density of clumped sites of all sizes is derived by allowing the maximum clump size to go to infinity and summing the mean number of clumps of all sizes,

$$\begin{aligned} \rho_C &= \sum_{n=1}^{\infty} \rho_N \frac{p_0(1-p_0)^{n-1}}{n} \\ &= \rho_N \frac{p_0 \ln p_0}{p_0 - 1} \end{aligned} \tag{4}$$

where $\ln(x)=\sum(x-1)^n/n$. By defining the nominal coverage as $\psi=\rho_N/\rho_0$, where $\rho_0=(\frac{1}{4}\pi\delta^2)^{-1}$ is the inverse area of each site, the ratio of clump density to individual site density, $\varepsilon=\rho_C/\rho_N$, can thus be compactly approximated by:

$$\varepsilon = \frac{4\psi}{\exp 4\psi - 1}. \tag{5}$$

We emphasize here that the above treatment is approximate and neglects some details of the overlapping statistics. Nonetheless, Eq. 5. has been found to reasonably describe the experimentally encountered under-counting problem [6] which is caused from the departure between clump density and site density. A more rigorous treatment, for example, can be based on Monte Carlo techniques[7] which can better address details in both variable overlap and voids, particularly important for arbitrarily shaped objects.

The behavior of Eq. 5 is shown in Fig. 2, where we plot the clumping ratio and the normalized clumping density (clumping coverage) as a function of nominal coverage. As is shown, the ratio of clumps to individual sites linearly departs from unity at low coverage, and approaches zero as the coverage increases. It is of interest to note that $\varepsilon\neq0$ when $\psi=1$ ($\varepsilon=0.075$) may be counter-intuitive, since this corresponds to a site density equal to the inverse size of the sites, but in face illustrates the random behavior of clumping: even at this exceedingly high density, a single huge clump is still not likely to occur. However, plotted along the right axis of Fig. 2 is the normalized clump density, which increases linearly at first and clumps are populated on the surface, but exhibits a characteristic peak at $\psi_p=0.4$, which corresponds to a maximum clumping coverage of 0.17. This peak at $\psi_p=0.4$ can be associated with the well-known 2D percolation threshold observed in condensed matter physics problems as well as in the study and containment of forest fires. For a nominal coverage above this threshold, the damage sites tend more and more towards one single clump.

Because ψ_p is uniquely determined by density (a function of fluence) and damage site size (typically a function of pulse length), we can use it as a rough limit, beyond which automated counting of sites is severely compromised by clumping. Still, even at this limit, the error associated with using clump density to estimate actual site density is greater than 50% (defined as $1-\varepsilon$).

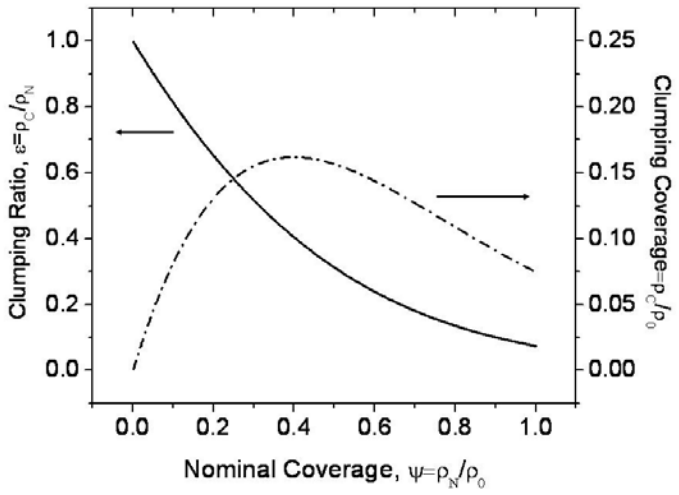

Figure 2: Plot of Eq. 5 (left axis), showing the continual decrease from unity towards zero of the ratio of clumps to individual sites, or equivalently, the compliment of the fractional error associated with using clump density to estimate individual site density. The right axis shows the clumping coverage, or normalized clump density, exhibiting a peak that corresponds to the percolation threshold of connected damage sites.

Using available λ=351 (3ω) nm data on fused silica exit surface damage site size versus Gaussian pulse length[8], which suggests $\delta \sim c\tau^{0.7}$ where $c=7\mu m/ns^{0.7}$, and a linear approximation for ε(ψ) at small ψ, we can estimate the associated counting error due to clumping as:

$$\%Error \approx 2.7\times10^{-4}\times\left[\tau(ns)\right]^{1.4}\times\rho(cm^{-2})\,. \tag{6}$$

This expression can be used as a reasonable approximation of the error due to undercounting up to about 35%. For example, the counting error would be about 20% for a 10ns pulse at a density of $\sim 3\text{x}10^3$ cm^{-2}, but would drop to less than 1% for 1ns pulses at the same density.

In terms of damage sites of unequal size, Armitage [4] first described the effect of a size distribution f(δ) on clumping, starting again with the Poisson probability of overlap between any two particles, and using instead the exact probability distribution function for randomly placed particles in a finite plane and approximating ε(ψ) for small clusters. Since the number of sites per unit area with diameters between δ' and δ'+dδ' ($0<\delta'<\infty$) is given by $\rho_N f(\delta')d\delta'$, the probability that a site of diameter δ does not overlap any sites in this differential range is now given by (see Eq. 1):

$$p_0 = \exp\left[-\pi(\delta+\delta')^2\rho_N f(\delta')d\delta'\right]. \tag{7}$$

By integrating over all sizes and ignoring moments of higher order than 2, it can be shown that ε can be expanded as

$$\varepsilon \approx 1-\pi\rho_N\left(\delta^2+\tfrac{1}{2}\sigma^2\right)+O\left(\psi^2\right) \tag{8}$$

where σ is the width of the size distribution. And by comparison with the first two terms of an expansion in ψ of Eq.5, we can approximate an effective ψ' as $\psi\rightarrow\psi'=\rho_N/\rho'_0$, where $\rho'_0=[\tfrac{1}{8}\pi(\delta^2+2\sigma^2)]^{-1}$ This approximation is valid as long as the damage site size distribution does not yield significant contributions from high-order moments, and in particular is a good approximation if $\delta^2>>2\sigma^2$ (see Fig. 3). Indeed, for the 3ns Gaussian data, 400 unclumped site diameters were determined to have an average size of 16μm and a

variance of 21 μm^2, thus justifying the approximation (see Fig. 3b). In the following treatment, we will assume an effective mean diameter equal to $\sim\sqrt{\delta^2+2\sigma^2}$.

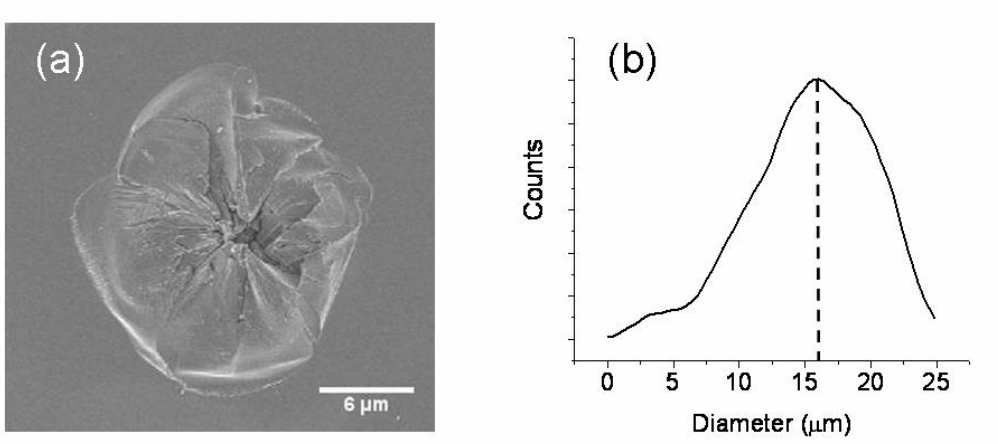

Figure 3: (a) Scanning Electron Microscope image of a single 3ns Gaussian-initiated damage site, showing the typical circular nature of the damage, and (b) an average-shifted histogram (ASH) plot of diameters for 400 individual damage sites (clumped sites were not counted).

PROBABILITY OF DAMAGE VERSUS FLUENCE

With the overlap statistics in hand, we now seek to modify the fluence dependence on (unclumped) damage sites as a function of fluence. Although several models exist to describe the probability distribution function[9,10], for simplicity and general agreement with our data, we choose the Weibull power-law distribution function, but in principle, other distribution functions could be applied here. It will be noted that in general, the density of observed damage sites increases quite rapidly with fluence, and can involve different so-called precursors that 'turn on' at different fluences (see for example Ref.10) We assume for simplicity that there exists a single precursor type/threshold and that, up to at least the onset of clumping, we do not encounter any saturation effects due to the unavailability of precursors beyond some density.

The Weibull distribution for damage site density as a function of fluence can be written as,

$$\rho_N(\phi) = a\phi^k \tag{9}$$

where a is a scaling constant, and the power k is typically in the range 5-12 [9] depending on the material. The exact physics leading to this somewhat empirical (statistical) description to the density function, to our knowledge, is yet to be specified. If the density of individual damage sites initiated on a surface as a function of fluence is given by Eq. 9, we can now express the density of clumps as a function of fluence that an automated microscope would observe as a function of fluence and mean site diameter:

$$\rho_C(\phi,\delta) = \varepsilon\left(\delta,\left[\rho_N(\phi)\right]\right)\rho_N(\phi) \tag{10}$$

Or explicitly in terms of the Weibull parameters,

$$\rho_C(\phi,\delta) = \frac{4\pi\delta^2 a^2\phi^{2k}}{\exp(4\pi\delta^2 a\phi^k)-1}. \tag{11}$$

We will refer to this function as the Weibull-Roach distribution, which combines actual physical origination of damage and observed effects that include clumping. One interesting thing to note is that, if the Weibull fit parameters are consistent above and below the percolation threshold, a fit can be applied

when error due to clumping is small, and then extended out to higher densities using only a single fitting parameter: δ. Alternatively, if the distribution of sizes is explicitly known (which may be difficult to determine when clumping is severe), one may, in principle, recover the true distribution of the damage precursors, even beyond the limit imposed by direct counting.

COMPARISON OF THEORY WITH ρ(ϕ) MEASUREMENTS

We now turn to the analysis of measured density estimates of damage initiations on fused silica exit surface following a single pulse of 351nm light. The details of the automated microscopy, thresholding algorithms and mapping to fluence images are described elsewhere[11]. 3 and 10ns single pulses averaging ~22 and ~50 J/cm^2 respectively were weakly focused (~f/20) onto two identical precision cleaned Corning 7980 fused silica surfaces. The 10ns beam spot was ~2cm diameter, while the 3ns beam spot was ~1cm diameter. Immediately after being shot in a 2.5 torr N_2 environment, samples were transferred in Class 100 conditions to the microscope for inspection. Roughly 60,000 damage 'blobs' were detected by automated microscopy for the 10ns pulse, while the number was about 10,000 for the 3ns sample.

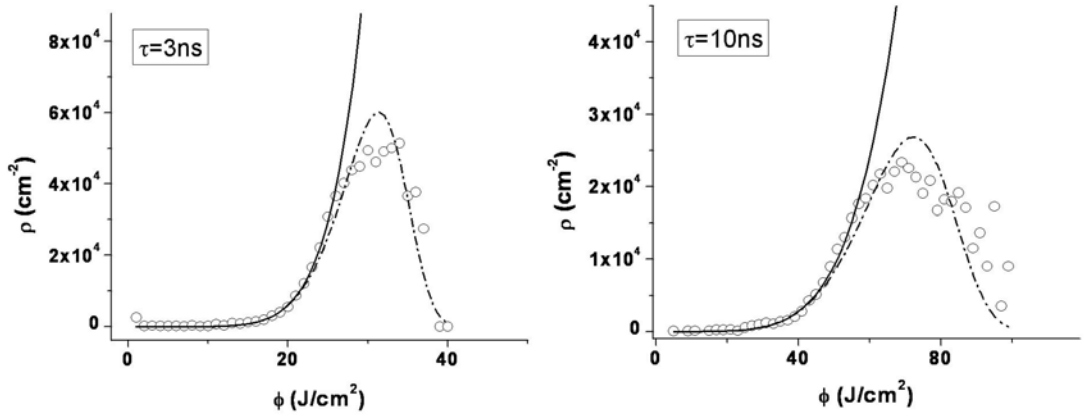

Figure 4: Observed density of damage sites versus fluence, ρ(ϕ) vs. ϕ, for 351nm, 3ns and 10ns Gaussian pulses (circles), compared with a Weibull power-law fit for ψ<0.1 (solid line), and the Weibull-Roach fit using the Weibull-only fit parameters, and fitting the single parameter δ (dash-dot line).

Figure 4 shows the results of the automated measurement, along with fits using Eqs. 9 and 11. As is evident in the 1-J/cm^2 binned data, a 'roll-over' or peak in density is observed for both 10 and 3ns, indicative of clumping. Also evident is the fact that, as described earlier, the onset of clumping occurs at lower densities (~2x10^5 cm^{-2}) in the 10ns case than in the 3ns case (~5x10^5 cm^{-2}), owing to the fact that the 10ns damage site diameters are roughly twice as large those of the 3ns sample. Shown with the data of Fig. 4 are results of the Weibull-only fit (solid lines), for 0<ψ<0.1 where the error due to clumping has been determined to be less than 10% over that entire range, and the full Weibull-Roach fit (dash-dot line) over the entire fluence range. The Weibull-Roach function was applied, using as fixed inputs the ψ<0.1 fit parameters (a, k), and as a variable input the damage site diameter, δ, resulting in an excellent fit to the data. In both cases, the extracted diameter (δ, fit) was in good agreement with that found directly by averaging over a number of unclumped sites (δ, meas.). Table I shows the results of the numerical fits.

Table I: Results of Weibull and Weibull-Roach fits of 3 and 10ns ρ(ϕ) data.

	a (cm^{-2})	k	δ, fit (μm)	δ, meas. (μm)	ψ_p	$\varepsilon(\psi_p)$
3ns	3.5x10^{-6}	7.1	~19	16	0.42	0.38
10ns	3.6x10^{-6}	5.6	~30	35	0.48	0.33

Because of the strong power dependence of the Weibull function, the peak associated with the percolation threshold at ψ_p=0.4 has shifted slightly to higher values in the W-R fit: ψ_p=0.42 and 0.48 for 3 and 10ns respectively. However, it should also be noted that the data appear slightly less steep near ψ_p as compared with the W-R fit.

One aspect that is important to emphasize about the experiment is that, along with errors due to the microscope thresholding algorithms inability to distinguish individual damage sites at high density, there is also a contribution to the error from inexact fluence registration to the damage site locations. Though not discussed at length here, distortions in the large beam image must be carefully measured and compensated in order to avoid such errors, as well as an effective method for sample-beam alignment. Errors from this effect could well contribute to the slight discrepancy of the data and the model.

INFLUENCE OF CLUMPING ERROR ON DAMAGE PROBABILITY CALCULATIONS

Although most Inertial Confinement Fusion lasers are not expected to operate at fluences and associated densities for typical fused silica where $\rho(\phi)$ measurements are complicated by clumping, such high fluence measurements are nonetheless useful in predicting damage when a so-called hotspot occurs. That is, if a coating flaw or other disturbance to the beam introduces sufficient phase modulation, and an optic resides near a focal point of this aberration, fluences can be as high as 30-40 J/cm^2. Figure 5 shows the intensification pattern caused from a coating flaw that was later removed from a conversion crystal upstream from a fused silica focusing element in a large aperture laser assembly. Care must be taken to identify such defects before the laser is fired, in order to mitigate their potential hazard or exchange the optic altogether. Thus, along with characterizing the phase perturbation a defect introduces to the beam and the resulting fluence levels at a particular optic, the damage probability at sometimes relatively high fluences must be known.

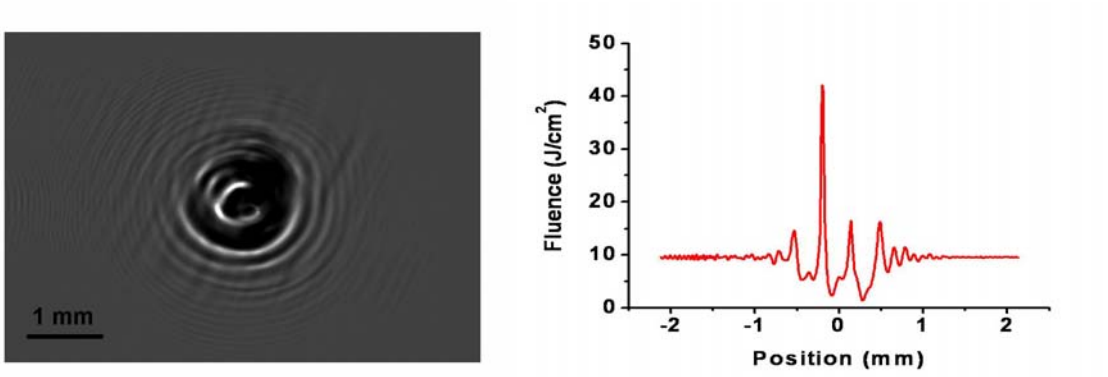

Figure 5: Intensification pattern projected onto an optical surface typical of an upstream coating flaw. The calculated image on the left was created by propagating 3ω light through a phase object several centimeters away. The lineout ro the right shows the peak intensity reaching as high as 40 J/cm^2.

Because the damage site initiation is generally believed to follow Poisson statistics, as discussed above, the probability $p(\phi)$ of finding any damage in an area A, given a mean density $\rho(\phi)$ of initiating sites is given by

$$p(\phi) = 1 - e^{-\rho(\phi)A}. \tag{12}$$

Hence, for large areas (e.g. entire ICF laser optical surfaces), only a modest density and therefore modest fluence will lead to finite probabilities of damage. It follows then that for very small areas, the fluence must be quite high for damage to be probable, simply owing the Poisson nature of the initiators. It is in this

regime precisely that undercounting errors in a measured $\rho(\phi)$ used in subsequent damage calculations will cause an *underestimate* of damage probability.

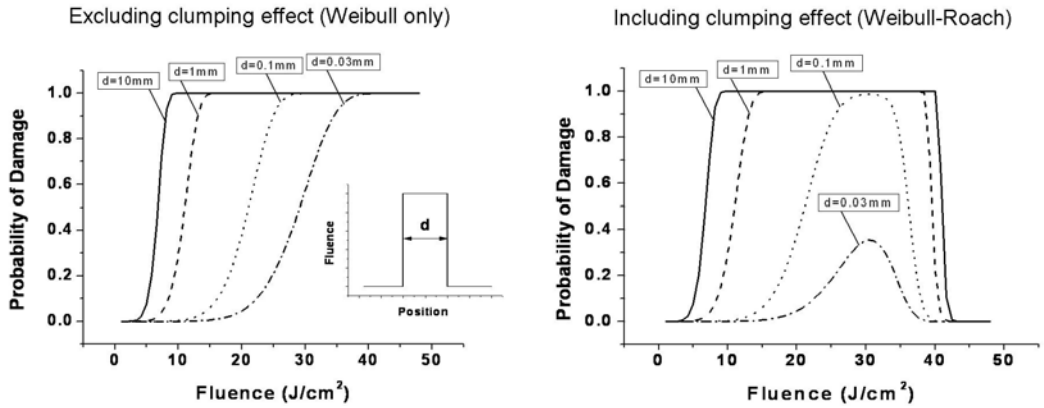

Figure 6: Effect of clumping on damage probability calculations based on measured $\rho(\phi)$. The roll-over in measured $\rho(\phi)$ at high fluence due to clumping (See Figure 4) causes an abnormal and non-physical prediction of damage probability for small beam sizes.

Figure 6 shows the effect of clumping on calculated probability curves using Eq. 12 as a function of fluence for a model 'hotspot' with a flat top profile of progressively decreasing diameter, from 1 cm down to 30 microns. If one assumes a single defect ensemble with a Weibull distribution function, the probability curves shift progressively to higher fluences as d is decreased, but always approaches 1 at some high fluence. However, when a Weibull-Roach distribution function is applied to simulate clumping error in the measured $\rho(\phi)$, a quite different behavior is observed at the smaller hotspot diameters. Just as there is a peak in the $\rho(\phi)$ curve due to undercounting, this peak also arises for the same reason in the $p(\phi)$ plots. Such an underestimate caused by density measurement errors could lead to incorrect characterization of certain hotspots, and subsequent unintended damage to optics.

Summary

While automated microscopy of large numbers of damage initiations continues to prove useful in characterizing laser-induced damage in optics, it is plagued by the problem of distinguishing individual damage initiations as the density grows large. Because of the subsequent under-counting associated with clumping, the $\rho(\phi)$ curves for fused silica damage at 3 and 10 ns show a characteristic and inevitable peak, which can be associated with the 2D percolation threshold of damage sites across the surface. The effect of random clumping on density estimates of fused silica exit surface damage can be theoretically described by combining Weibull statistics for damage density versus fluence and a simple model for clumping of randomly placed objects as function of density. Using this model, damage site sizes could be extracted, further validating this approach, and key parameters associated with the clumping effect evaluated. A rough estimate of the error versus pulse length and density for exit surface fused silica damage at 3ω was derived, and can be used to quantify the undercounting error at any point along the $\rho(\phi)$ curve, and establish bounds to the data validity. Using a Weibull-Roach model for clumping, the effect of undercounting on damage probability estimates was then explored, where it was shown that, for small area 'hot spots' in a beam on the order of 30-100 μm, and fluences near 40 J/cm^2, undercounting of $\rho(\phi)$ can lead to an underestimate of damage probability.

REFERENCES

1. E. I. Moses EI. **"**The National Ignition Facility: status and plans", 2005 IEEE Int. Conf. on Plasma Sci. - ICOPS 2005 (IEEE Cat No. 05CH37707) 1 (2005)

2. W. A. Massey, "The analysis of queues with time-varying rates for telecommunication models" Telecom. Systems 21(2-4), 173 (2002).

3. F. Garwood, "The variance of the overlap of geometrical figures with reference to a bombing problem" *Biometrika* 34, 1 (1947).

4. P. Armitage, "An overlap problem arising in particle counting" *Biometrika* 36, 257 (1949).

3. C. Mack, "On clumps formed when convex laminae or bodies are placed at random in two or three dimensions" *Proc. Camb. Phil. Soc.* 52 246 (1956).

5. S.R. Broadbent, J.M. Hammersley, Proc. Camb. Philos. Soc. 53 (1957) 629.

6. S. A. Roach, *The Theory of Random Clumping*, Methuen Press, London, 1968.

7. A. M. Kellerer, "Counting figures in planar random configurations" *J. Appl. Prob.* 22, 68 (1985).

8. C. W. Carr, M. J. Matthews, J. D. Bude and M. L. Spaeth, Proc. Of SPIE, 6403, 64030K-1 (2006).

9. R. H. Picard, D. Milam, and R. A. Bradbury, "Statistical analysis of defect-caused laser damage in thin films" *Appl. Opt.* 16(6) 1563 (1977).

10. J.O. Porteus and S. C. Seitel, "Absolute onset of optical surface damages using distributed defect ensembles" *Appl. Opt.* 23(21) 3796 (1984).

11. C. W. Carr, M. D. Feit, M. C. Nostrand, and J. J. Adams, "Techniques for qualitative and quantitative measurement of aspects of laser-induced damage important for laser beam propagation"
Meas. Sci. & Tech. 17(7) 1958 (2006).

This work performed under the auspices of the U.S. Department of Energy by Lawrence Livermore National Laboratory under Contract DE-AC52-07NA27344. UCRL-PROC-236247